AIMS Energy, 9(2): 193–212.
DOI: 10.3934/energy.2021011
Received: 02 July 2020
Accepted: 09 December 2020
Published: 15 January 2021

http://www.aimspress.com/journal/energy

Research article

Comparative analysis of apple and orange during forced convection cooling: experimental and numerical investigation

Taliv Hussain*, Mohd Ahsan Kamal and Adnan Hafiz

Mechanical Engineering Department, Aligarh Muslim University, Aligarh, India, 202002

* **Correspondence:** Email: hussaintaliv@gmail.com; Tel: +919720229876.

Abstract: The main theme of this paper is to make improvements in heat transfer during cooling of food products in forced convection environment. In the present study the effect of air velocity during precooling of spherical food products i.e., apple and orange is seen. The experiments are performed on an air blast apparatus and results are compared using simulation with a 3D CFD model. Models are developed and solved with the later one more likely to be close to experiments and hence this model is studied at 5 different velocities (0.5, 1.0, 2.0, 2.5 and 3.0 m s^{-1}) for both samples. It is observed that cooling is improved significantly up to a particular speed for both apple and orange and increasing the speed above their respective critical speeds i.e., 2.5 m s^{-1} for apple and 2.0 m s^{-1} orange, does not enhance the cooling significantly and hence is not advisable to increase the speed above their critical speed as it leads to loss of energy which in turn increases the overall operational cost. The half cooling time and the seven-eight cooling time consequently decreases by 45.91% and 44.61%, respectively, for an individual apple with an increase in air-inflow velocity from 0.5 to 3.0 m/s and 44.27% and 43.31% respectively for orange. The food sample is rotated about its axis slowly at 2 rad s^{-1} and its effect is also seen. It is observed that there is significant amount of increase in the cooling rate and also the cooling is uniform.

Keywords: forced convection; simulation; cooling; spherical food products; half cooling time and seven-eight cooling time

Nomenclature: *Bi*: Biot Number; c_p: Specific Heat Capacity of air (J $kg^{-1}K^{-1}$); *h*: Heat Transfer Coefficient ($Wm^{-2}K^{-1}$); *Nu*: Nusselt Number; *Pr*: Prandtl Number; *Re*: Reynolds Number; *T*: Temperature (K); *t*: Time (sec); *r*: radial distance (m); *W*: Water Content; α: Thermal Diffusivity (m^2s^{-1}); ζ: Fourier Number; A: Surface area (m^2); C: Cooling coefficient (min^{-1}); F_1: Blend function; HCT:

Half cooling time (min); J: Lag factor; Re: Reynolds number; H: Relative humidity of air; RMSE: Root-mean-square error (C); RD: Relative deviation (%); S: Source term (kg $m^{-2}s^{-2}$); SECT: Seven-eights cooling time (min); U: Velocity vector (m s^{-1}); u,v,w: Air velocity components in x, y and z directions (m s^{-1}); u_i, u_j: Mean velocity components in x and y (m s^{-1}); x_i, x_j: Cartesian coordinates (m); ρ: density (kg m^{-3}); k: thermal conductivity (W $m^{-1}K^{-1}$); μ: dynamic viscosity (Pa s); μ_t: turbulent viscosity (kg m^{-3}); κ: turbulent kinetic energy (m^2s^{-2}); δ_{ij}: kronecker delta; ω: specific dissipation rate (s^{-1}); D: mass transfer coefficient (kg m^{-2}Pa s^{-1}); ε: Latent heat of vaporisation of water (J kg^{-1})

1. Introduction

In India nearly 30% of the perishable items goes waste due to the lack of proper preservation facilities. More over in developing countries only a limited quantity of fruits and vegetables are produced for local markets or for exportation due to lack of machinery and infrastructure. Reduction of high wastage of fruits and vegetables entails various measures to be adopted to minimise these losses during harvesting, handling, storage, packaging and processing of fresh fruits and vegetables into suitable products with improved storage characteristics. The cold preservation is the most suited technique for the preservation of fruits, vegetables and flesh food products as it retains their original flavour, aroma and texture. Refrigeration controls microbiological, biochemical and physical processing of the food products and thus prevents deterioration and increases storage life. It is very necessary for the producer to remove the field heat from the grown fruits and vegetables to improve the economic performance across the entire cold chain [1]. This insures the proper handling of the produce and reduces the losses. The requirement of low temperature does not ends here the temperature need to be maintained low throughout the journey till the fruit is in the hands of the ultimate buyer buying for his consumption. It is not possible to consume the produce right after it is harvested it takes time for the produce to be consumed so an extended shelf life is required. Preservation does this work of improving the shelf life to two days in some fruits to ten days. Thus it is important to increase the shelf life of the produce. As the time proceeds the quality of the perishable products deteriorates and hence preservation of those qualities become necessary [2]. The critical step in retaining the quality is precooling after harvest to remove field heat. Precooling helps in the reduction of respiration rate and enzymatic activities. It also retards microbial growth and thus delays the deterioration of produce [3]. By precooling moisture loss is minimised and reduction in the ethylene production is allowed and thus this delays the ripening and finally enhances the quality and shelf life. There are basically two techniques of pre-cooling. They are forced air precooling and water cooling. Both the techniques have their own advantages and disadvantages. In forced air precooling air is used for cooling. In this cold air at a certain velocity is flown over the product. The temperature of the air is maintained with the help of an external refrigeration cycle using a refrigerant to cool the air. A centrifugal fan is used to force the air on the fruit in forced air cooling method whereas water is used in water cooling in place of air. Air is in abundance and water is limited so air cooling is preferred over water cooling. Also the chilling losses are less in air as compared to water cooling. So most commonly used is forced air pre cooling [4]. In recent years with the advancement in computer technology CFD has emerged as the most important numerical technique to solve the physical problem. Complex geometries can be solved with ease using CFD. The results obtained using CFD are realistic and close to experimental results. They provide an

Engineer a wide range of options to lessen the assumptions and move to a more accurate solution to the physical problem. At present it is most growing field of research and in almost every field it has its reach. In cooling application it is a challenging task to maintain the uniformity in cooling and simultaneously the energy conservation. Cooling uniformity is necessary to prevent the fruit from chilling injuries and energy conservation is required to reduce the cost of preservation. CFD provide 3-D temporal and spatial distribution of produce during precooling [5]. This distribution is helpful is predicting the thermo physical properties of the fruits. It provides a variety of options for the users and is user friendly. Simultaneous study of air flow and heat transfer during forced cooling is possible with the CFD. Optimisation between cost and quality is important. Fast cooling without the chilling injury is required. Cooling rate and uniformity depend upon several factors such as size, shape, thermal properties, air flow rate, cooling temperature and accessibility of cooling air to produce. The operational cost of the system is combined energy consumption by refrigeration system and the fan which maintains airflow. A significant amount of energy is consumed by the fan. Thus this cost must be reduced to minimum and this in turn reduces the post-harvest losses. There is deterioration of food quality after harvest which need to be preserved. This is done by cooling the food sample from the farm filed temperature to optimal temperature of storage. One of the most significant application of refrigeration industry is in the preservation of perishable food products. The fruits and vegetables are the best carriers of vitamins, essential fibres, antioxidants which are important from nutritional health of human being [6]. In India nearly 30% of the perishable items goes waste due to the lack of proper preservation facilities. Moreover in developing countries only a limited quantity of fruits and vegetables are produced for local markets or for exportation due to lack of machinery and infrastructure. Reduction of high wastage of fruits and vegetables entails various measures to be adopted to minimise these losses during harvesting, handling, storage, packaging and processing of fresh fruits and vegetables into suitable products with improved storage characteristics [7]. The cold preservation is the most suited technique for the preservation of fruits, vegetables and flesh food products as it retains their original flavour, aroma and texture. Refrigeration controls microbiological, biochemical and physical processing of the food products and thus prevents deterioration and increases storage life.

Albayati et al. [8] studied the effect of air velocity on the temperature profile of the food product.They used apple,papaya and grape as the sample food product which were cooled by blowing air at velocities 1.6, 2.3, 3.3, 4 m s^{-1}. Three positions i.e., at R = 0, R = d/2 and R = d/4 were choosen and cooling curves were drawn for these positions and they observed that for all the three positions the curve was exponential.The heat transfer coefficient of three samples were improved significantly and the precooling time was reduced and hence less energy consumption. Ansari et al. [9] solved 1-D transient heat conduction equation in spherical coordinates using convective surface boundary condition during air cooling. He included the cooling effect of dessication (process of extreme drying) using the enthalpy potential concept. In their calculation scheme they proposed that upto half cooling time both heat and mass transfer and after that only heat transfer is taking place.This scheme was in good agreement with the experimental results for all the samples under the investigation. Ansari and Afaq [10] gave a new method of measuring thermal diffusivity of spherical produce. Numerically generated time temperature data was used for homogeneous spherical produce and a relationship between Fourier No., Biot No., dimensionless radial distance and Normalized temperature was developed. This developed method was used for the thermal diffusivity measurement of apple, oranges and potatoes. Ambaw et al. [11] developed a direct model based on

explicit geometry of stacked products. They used a 3-D FV CFD model for their study. Simulations were carried with an unstructured tetrahedral mesh by the help of ANSYS-CFX. Convection-Diffusion-Absorption model parameters were applied. Bairi et al. [12] gave a simple method for the calculation of the thermal diffusivity of different sample of food. It was based on the analytical solution of 1-D Fourier equation applied to a cylinder. Thermal diffusivity calculated using this method were very precise and an error of about 4% was obtained. Chuntranuluck et al. [13] used the FDM in order to simulate the conditions of unsteady state cooling of sphere, infinite slabs and infinite cylinder shape of food materials subjected to both convection as well as evaporation at the product surface. Simulations were performed by varying air temperature, surface heat transfer coefficient, product initial temperature, surface water activity and relative humidity of air. Algebraic equations were proposed to find parameters like product equilibrium temperature as time, a slope parameter of semi-log plots and an intercept parameter of the same plot. The first equation was based on the psychometric theory and the other two equations were derived using non linear regression. It was found that the numerically simulated cooling times were predicted within ±5%. Defraeye et al. [14] used CFD for the evaluation of forced convection cooling of orange. Their focus was on fruit cooling rate as well as system energy consumption. They proposed new package design both showed improved cooling rate and cooling uniformity. Dehghanya et al. [15] gave a detailed mathematical modelling procedure for the airflow heat and mass transfer occurring during forced convection cooling of produce in order to optimise the cooling process. They explored two main modelling procedures i.e., PMA and DNS and a process was optimised using DNS approach. Delele et al. [16] developed a 3-D CFD model of air flow and heat transfer process inside a packed horticulture produce. They observed that the airflow and the temperature inside the produce bulk were heterogeneous. Denys et al. [17] studied transient temperature and albumen velocity profiles during thermal pasteurization of intact eggs with the help of a CFD package. They observed that in white fraction only convective heat transfer occurred where as in yolk only conductive heat transfer occurred. Hussain, and Ansari [18]. The specific heat capacity increases with the increment in the percentage of moisture quantity as in cucumber, it was 96% and in banana, it was 74%. The thermal conductivity of cucumber was found to be 18.7%, 7.6%, 5.1% more than that of banana, orange, capsicum respectively in case of free convection cooling but it was 18.7%, 7.8%, 5.3% more than that of banana, orange, capsicum respectively in case of forced convection cooling. In free convection cooling, the value of thermal diffusivity of cucumber was noted to be 9.02%, 2.96%, 3.85% more than that of banana, orange,capsicum respectively while in case of forced convection cooling, it was 76.06%, 62.62%, 20.19% more than that of banana, orange, capsicum respectively. Ghiloufi and Tahar [19] the model SST k–ω is used to analyze the air turbulences. For normal design of the cold store room and during a precooling period of 40 h, the air velocity and temperature are determined in the different locations inside the room and vary between 0.25–7 m/s and 3–6 °C. While the product temperature remains higher than the required storage conditions of about 12 °C. A new cold store room design is proposed using specific aerodynamic air deflector profiles. That permits to improve the heat transfer between the cold air and product.

2. Objective of the research

The aim of the present work is to develop a 3-D CFD model of the spherical food products kept under a forced convection cooling environment. This model is validated experimentally. The

experiments are performed in the lab on air blast apparatus. The simulations are run at 5 different velocities and time-temperature data are obtained. They are plotted on a graph to see the effect of the different velocities. It is performed for spherical food products i.e., orange and apple. Also the produce is rotated at its axis and time-temperature data is obtained and is compared with the case of produce cooling without rotation. Thus the effect of velocity on cooling as well as the effect of rotation are studied in this paper.

3. Experimentation and simulation

Experiments (Figure 1) were carried out on spherical shaped food samples (orange and apple). Experimental measurement of transient time temperature behaviour during pre-cooling of these food products is done, with approximately spherical geometry forced cooling environment.

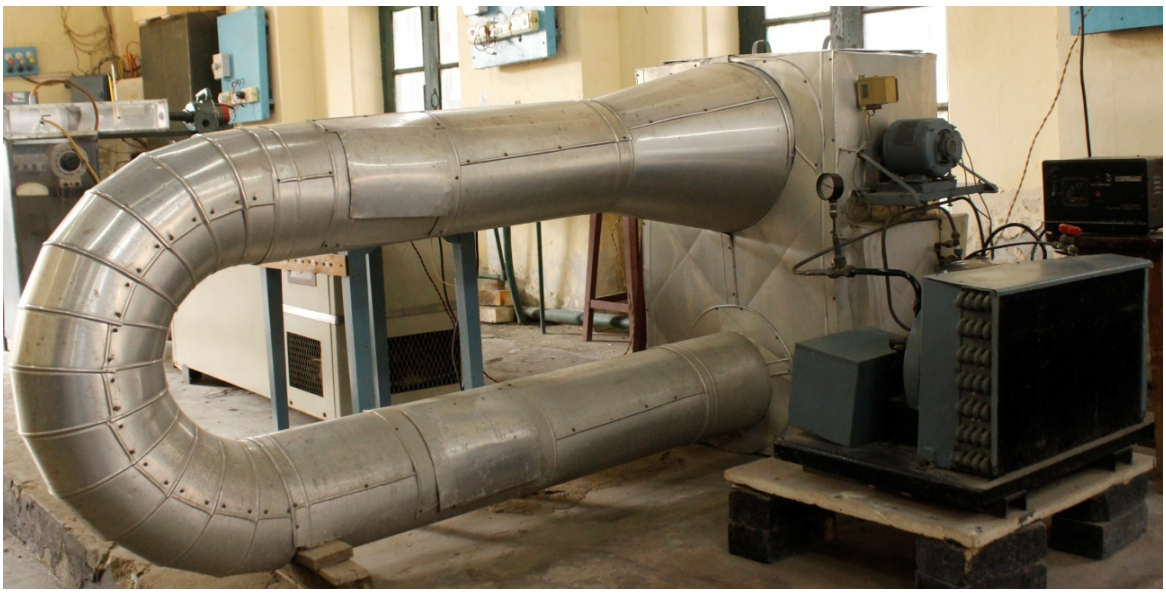

Figure 1. U-Duct for forced convection cooling.

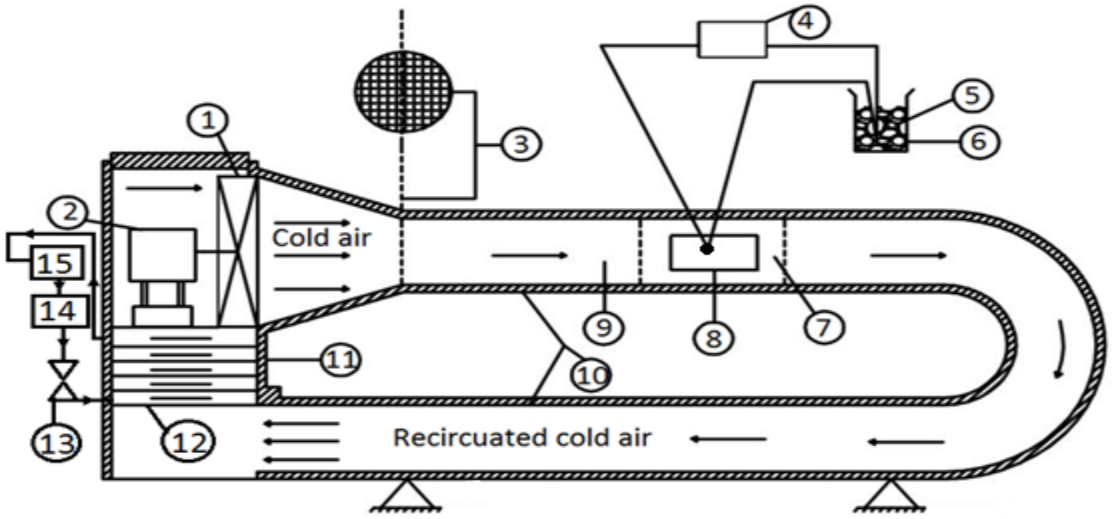

Figure 2. Line diagram for forced convection system. 1. Blower; 2. Motor; 3. Iron Grid; 4. Thermocouples; 5. Ice; 6. Thermos Flask; 7. Test Section; 8. Food Sample; 9. Cooling Duct; 10. Insulation (Glass Wool); 11. Insulation (Thermo-Freeze); 12. Cooling Coil; 13. Expansion Device; 14. Air Cooled Condenser; 15. Compressor.

The forced convection simplified diagram is shown in Figure 2, which comprises of a chilled air duct with vapour compression refrigeration system and air blower, milli-voltmeter, anemometer, copper-constantan thermocouple.

- 1.06 m × 0.6 m × 0.4 m refrigerated bunker consists of 22 S.W.G galvanised iron sheet with 0.2 m dia hole at the bottom end and a 0.4 m dia hole at the top.
- A tapered duct 0.45 m long from the upper hole was attached and itsanother portion with a 0.2 m dia closed duct. Overall duct was then further covered by around 3 cm thick glass wool.
- For circulation of air blower was used. A particular air velocity was kept when the refrigeration system was started and repeatedly was flowed through the cooling coils of the R-22 VCR system.

The copper constantan thermocouple was used for temperature measurement which is connected to a data logger. The blower was used for air circulation. The air speed was maintained at around 4.34 m/sec when the refrigeration system was started and was recirculated again and again across the cooling coils of the refrigeration system. In forced convection cooling, we first run the vapour compression refrigeration system and air blower in the U-duct until a steady low temperature is reached inside the duct. The sample was suspended with the help of specially fabricated frame and hook in the test section. Product temperatures were measured using copper constantan thermocouples. These thermocouples were inserted in the food product radially. The temperature was measured until the temperature approaches the temperature of cooling medium with an interval of one minutes. The time and temperature were recorded for orange and apple. Table 1 shows measuring instruments with their specifications and accuracy.

Table 1. Measuring Instruments with their specifications and accuracy.

S.No.	Devices	Specification/Range	Accuracy
01	Voltmeter	0–300 V	±0.02 V
02	Ammeter	0–5 A	±0.02 A
03	Temperature Sensor	RTD PT-100/3W/-50 to 400 Celsius	±0.1 Celsius
04	Pressure gauge	Discharge-0 to 300 psi Suction-30 to 150 psi	±0.0375

3.1. Modelling 3D

In this study, a 3D computational fluid dynamics modelling of a spherical shape food sample and air around it was done. The governing differential equations describing the fluid flow were solved with a fluid-flow solver Fluent 16.0 in the 3D computational domain. The solution domain was subdivided into a number of discrete control volumes, and the solution method involved solving each differential equation in a sequential manner through transient turbulence simulations with a second-order implicit time integration scheme. We used transient simulations to simulate the regularity of the temperature change of the sample fruit during precooling. The domain had two distinct subdomains: a free-airflow zone and a produce zone (i.e., the air and sample). To simplify our calculation and describe the experimental system, following assumptions were made:
(1) The air is considered to be an incompressible fluid with constant properties;
(2) The air is observed as a Newtonian fluid;
(3) We ignored radiation between the sample and the air;
(4) The experimental instruments have a no effect on airflow;

3.2. Governing equations

The flow in the free-airflow zone was solved by using the Reynolds-average Navier-Stokes equations.
Conservation of mass

$$\frac{\partial \rho_a}{\partial t} + div(\rho_a U) = 0 \tag{1}$$

Conservation of momentum

$$\frac{\partial(\rho_a u)}{\partial t} + div(\rho_a u U) = div(\mu_a grad u) - \frac{\partial p}{\partial x} + [-\frac{\partial(\rho_a \overline{u'^2})}{\partial x} - \frac{\partial(\rho_a \overline{u'v'})}{\partial y} - \frac{\partial(\rho_a \overline{u'w'})}{\partial z}] + S_u, \tag{2}$$

$$\frac{\partial(\rho_a v)}{\partial t} + div(\rho_a v U) = div(\mu_a grad v) - \frac{\partial p}{\partial y} + [-\frac{\partial(\rho_a \overline{u'v'})}{\partial x} - \frac{\partial(\rho_a \overline{v'^2})}{\partial y} - \frac{\partial(\rho_a \overline{v'w'})}{\partial z}] + S_v, \quad (3)$$

$$\frac{\partial(\rho_a w)}{\partial t} + div(\rho_a w U) = div(\mu_a grad w) - \frac{\partial p}{\partial z} + [-\frac{\partial(\rho_a \overline{u'w'})}{\partial x} - \frac{\partial(\rho_a \overline{v'w'})}{\partial y} - \frac{\partial(\rho_a \overline{w'^2})}{\partial z}] + S_w, \quad (4)$$

Conservation of energy

$$\frac{\partial(\rho_a T)}{\partial t} + div(\rho_a U T) = div(\frac{k_a}{c_{p,a}} grad T) + [-\frac{\partial(\rho_a \overline{u'T'})}{\partial x} - \frac{\partial(\rho_a \overline{v'T'})}{\partial y} - \frac{\partial(\rho_a \overline{w'T'})}{\partial z}] + S, \quad (5)$$

where ρ_a is the air density (kg/m^3), t is time (s), U is the velocity vector (m/s), u, v and w are the air velocity components (m/s) in the direction of x, y and z, respectively, p is the fluid pressure (N/m^2), λ_a is the thermal conductivity of cooling air (W/mK), μ_a is the dynamic viscosity (Pa s), $c_{p,a}$ is the air-specific heat capacity (J/kgK) and S_u, S_v and S_w represent the source terms in the direction of x, y and z directions, respectively. This work does not consider source term effect so $S_u = S_v = S_w = 0$, $\overline{u_i' u_j'}$ is the specific Reynolds stress term and i and j are the Cartesian coordinates. The complete equation is

$$\overline{u_i' u_j'} = -\mu_t(\frac{\partial u_i}{\partial x_j} + \frac{\partial u_j}{\partial x_i}) + \frac{2}{3}(\rho_a \kappa + \mu_t \frac{\partial u_i}{\partial x_i})\delta_{ij}, \quad (6)$$

where μ_t is the turbulent viscosity (kg/m^3), u_i and u_j are the mean velocity components in the x, y and z directions (m/s), x_i and x_j are the Cartesian coordinates (m), κ is the turbulent kinetic energy (m^2/s^2), δ_{ij} is the Kronecker delta ($\delta_{ij} = 1$ when I = j, otherwise $\delta_{ij} = 0$).

3.3. Initial conditions and boundary conditions

The spherical shape fruit initial temperature and the cooling-air temperature were 300 K and 275 K, respectively. At the walls of the domain no slip and no penetration boundary conditions are used. Moreover, Inflow, outflow and Air sample interface boundary conditions are as follows:

Inflow Boundary: The velocity-inlet boundary conditions are used to define the airflow velocity at the inflow boundary. The airflow velocity is set by using five different air-inflow velocities: 0.5, 1.0, 2.0, 2.5 and 3.0 m s^{-1}, and the air-inflow temperature is taken as the cooling air temperature (275 K).

Outlet Boundary: Outflow boundary conditions are adopted at the outlet boundary because in this case it is assumed that the flow is fully developed and there is no velocity gradient in the direction of flow.

Air-sample Interface: Coupled boundary conditions are used at the air-sampleinterface. At the air-apple interface, no-slip and continuity boundary conditions are applied.

3.4. Discretization and analysis of mesh sensitivity

Figure 3 shows the geometry of sample along with the domain. Table 2 shows domain independence, Table 3 shows grid independence and Table 4 shows time step independence. After studying the sensitivity of the results with respect to the mesh, meshes with a maximum edge length of 6.5 mm are found to be optimum. Reduced size mesh cells led to the same results for the simulation but increased the computation time. Therefore, the geometry was discretized into an unstructured mesh of 542930 cells.

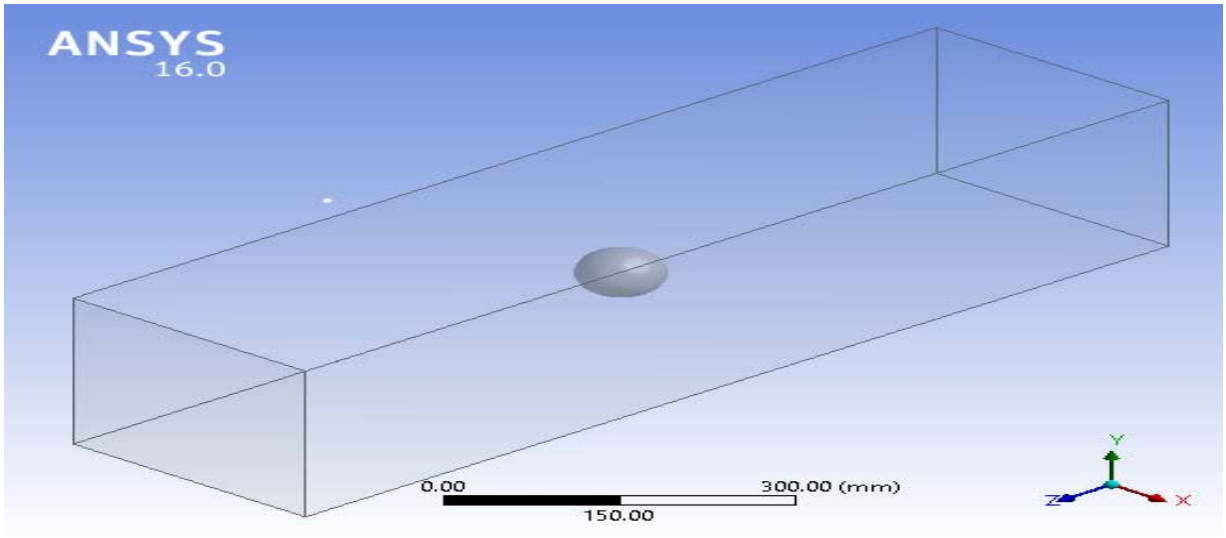

Figure 3. Geometry of sample along with the domain.

Table 2. Domain independence.

Domain Size	H (W $m^{-2}K^{-1}$)	Nu
3 d × 3 d × 8 d	31.20	104
5 d × 5 d × 12 d	31.60	105.34
5 d × 5 d × 16 d	31.86	106.20
7 d × 7 d × 12 d	31.80	106

Table 3. Grid independence.

Grid size (mm)	No of cells	H (W $m^{-2}K^{-1}$)	Nu
7	457377	30.22	100.73
6.5	542930	31.60	105.34
6	675082	31.68	105.60

Table 4. Time step independence.

Time step (s)	H (W $m^{-2}K^{-1}$)	Nu
30	31.60	105.34
60	31.63	105.43

Equations 7 & 8 is used in this CFD Analysis by using Semi-implicit method for pressure-linked equations (SIMPLE) to couple pressure to velocity and the second-order upwind scheme for the convection terms were used, which describe flow and turbulence. We imposed a convergence criterion of 10^{-4} for continuity, momentum and turbulence and 10^{-6} for the energy equations. The SST κ-ω turbulence model gave better accuracy and convergence as compared to the other two-equation turbulence models that were used (standard k-E, RNG k-E and standard κ-ε) as quoted in research. As a result, the SST κ-ω turbulence model was used in this study [19].

$$\frac{\partial(\rho_a k)}{\partial t} + \frac{\partial}{\partial x_j}(\rho_a U k) = \frac{\partial}{\partial x_j}[(\mu + \frac{\mu_t}{\sigma_{k3}})\frac{\partial k}{\partial x_j}] + Pk - \beta^* \rho_a k\omega + Pkb, \tag{7}$$

$$\frac{\partial(\rho_a \omega)}{\partial t} + \frac{\partial}{\partial x_j}(\rho_a U \omega) = \frac{\partial}{\partial x_j}[(\mu + \frac{\mu_t}{\sigma_{k3}})\frac{\partial \omega}{\partial x_j}] + 2(1-F_1)\rho_a \frac{1}{\sigma_{\omega 2}}\frac{\partial k}{\partial x_j}\frac{\partial \omega}{\partial x_j} + \alpha_3 \frac{\omega}{k} Pk - \beta \rho_a \omega^2 + P_{\omega b}, \tag{8}$$

where μ (Pa s) is the dynamic viscosity, k (m^2/s^2) is the turbulent kinetic energy; ω is the specific dissipation rate in s^{-1}, F_1 is a blend function and β* = 0.09. The constants σ_{k3}, β, $\sigma_{\omega 2}$ and α_3 are correlated with the blend function F_1, and P_k, P_{kb} and $P_{\omega b}$ are intermediate variables. Table 5 shows the input parameters.

Table 5. Input parameters.

Parameters	Value	
	Apple	Orange
ρ_a (kg/m^3)	1.2876	
μ_a (Pa s)	1.7276×10^{-5}	
$c_{p,a}$ (J/kgK)	1004.8	
ρ_s (kg/m^3)	837.22	960
$c_{p,s}$ (J/kgK)	3821.96	3850
k_s (W/mK)	0.4508	0.3860
d (mm)	80	80

4. Results and discussions

4.1. Experimental observation for APPLE and ORANGE in forced convection environment

The Figures 4–6 show the variation of temperature with time at 3 different velocities at 3 different locations (R = 0, R = R/4, R = R/2) for oranges, the velocities chosen in this case also show the approximate comparison with velocities taken in kumar et al. [20] and it is seen that the cooling time increases upto 5–15 minutes for relatively lower velocity. Figures 7–9 show the variation of temperature with time at 3 different velocities at 3 different locations (R = 0, R = R/4, R = R/2) for apples and it is seen that for moderately lesser velocity the cooling time is higher for 6–12 minutes.

The effect of velocity is more profound in case of oranges. Figures 10 and 11 Shows the validation 3-D CFD model with the experimental results for orange and apple respectively at a velocity of 3.0 m s^{-1}.

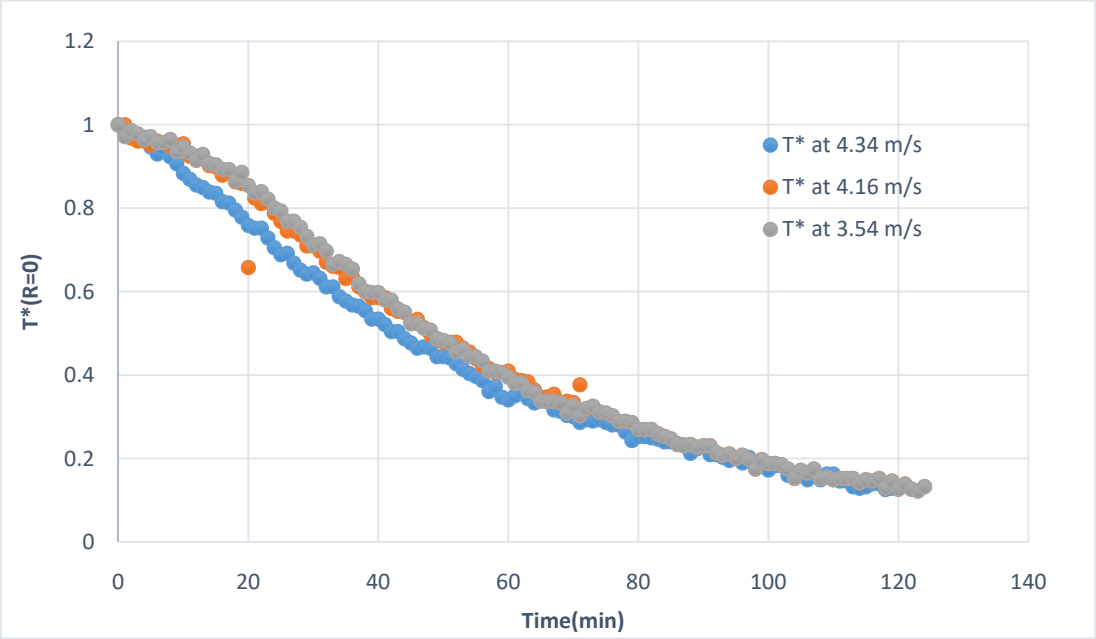

Figure 4. Variation of non-dimensional temperature with time for orange at 3 different velocities.

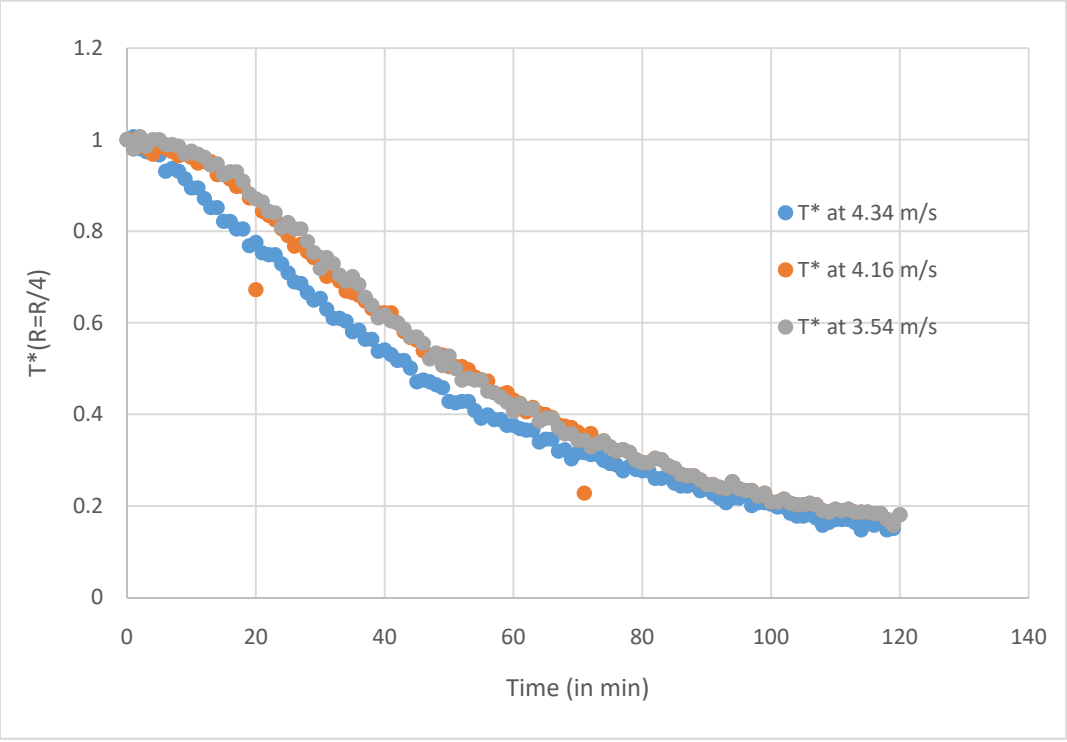

Figure 5. Variation of non-dimensional temperature with time for orange at 3 different velocities.

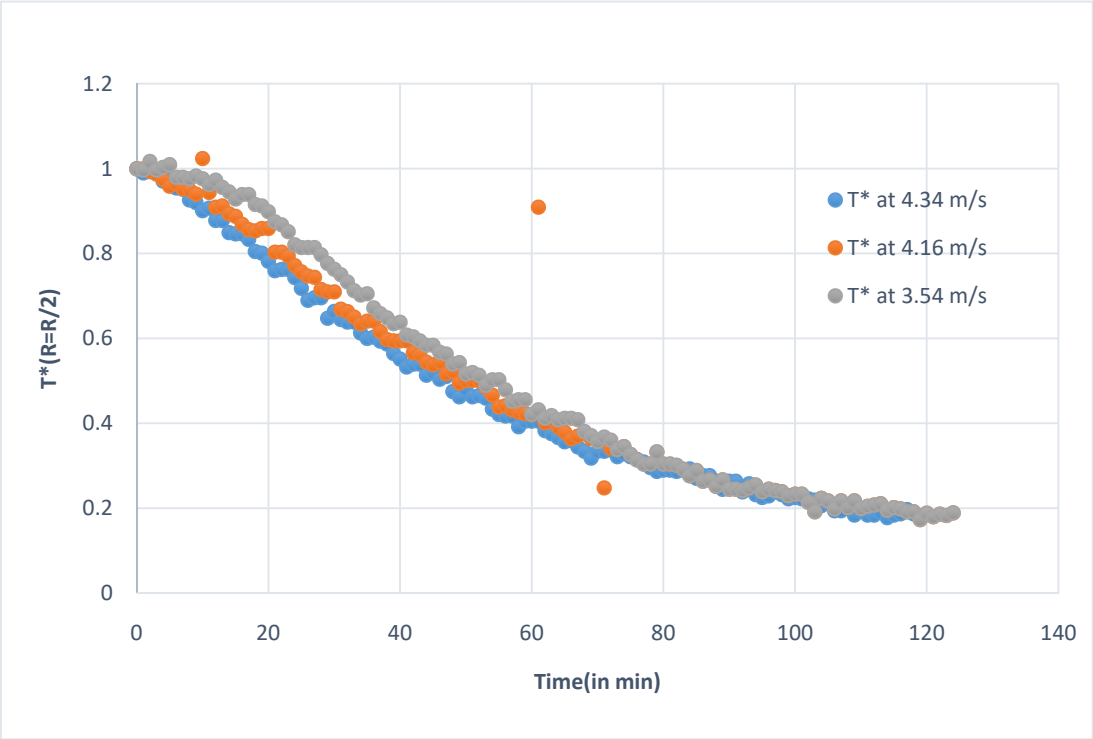

Figure 6. Variation of non-dimensional temperature with time for orange at 3 different velocities.

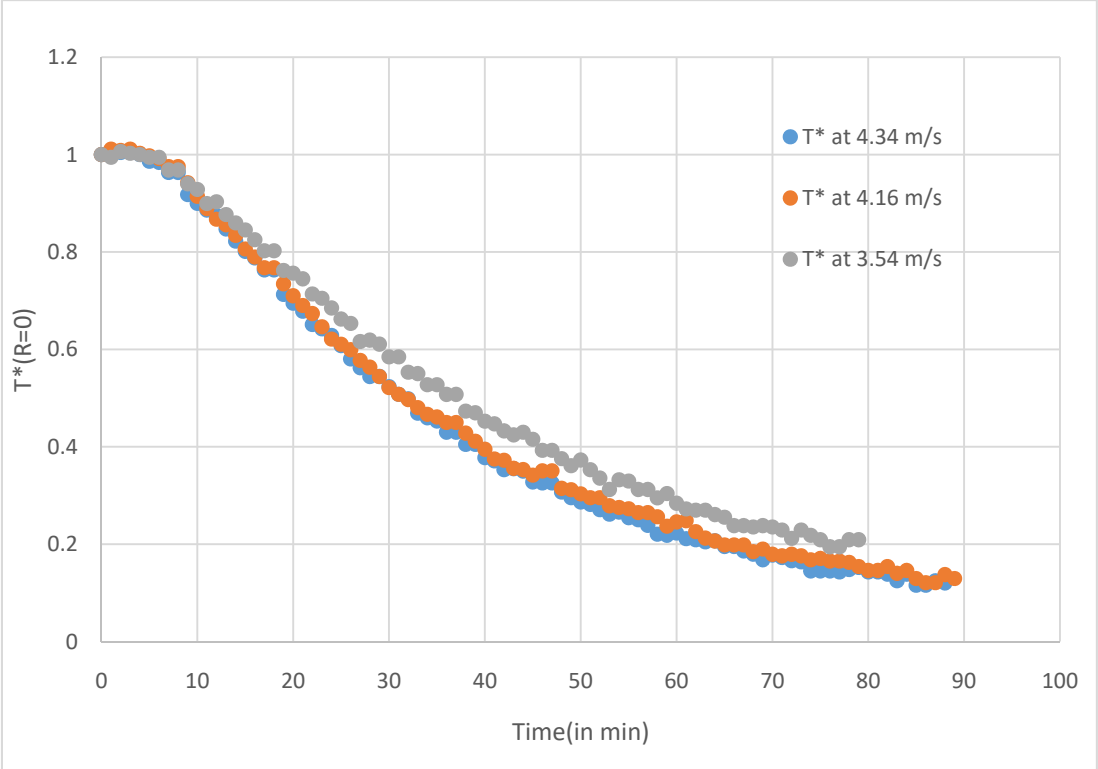

Figure 7. Variation of non-dimensional temperature with time for apple at 3 different velocities.

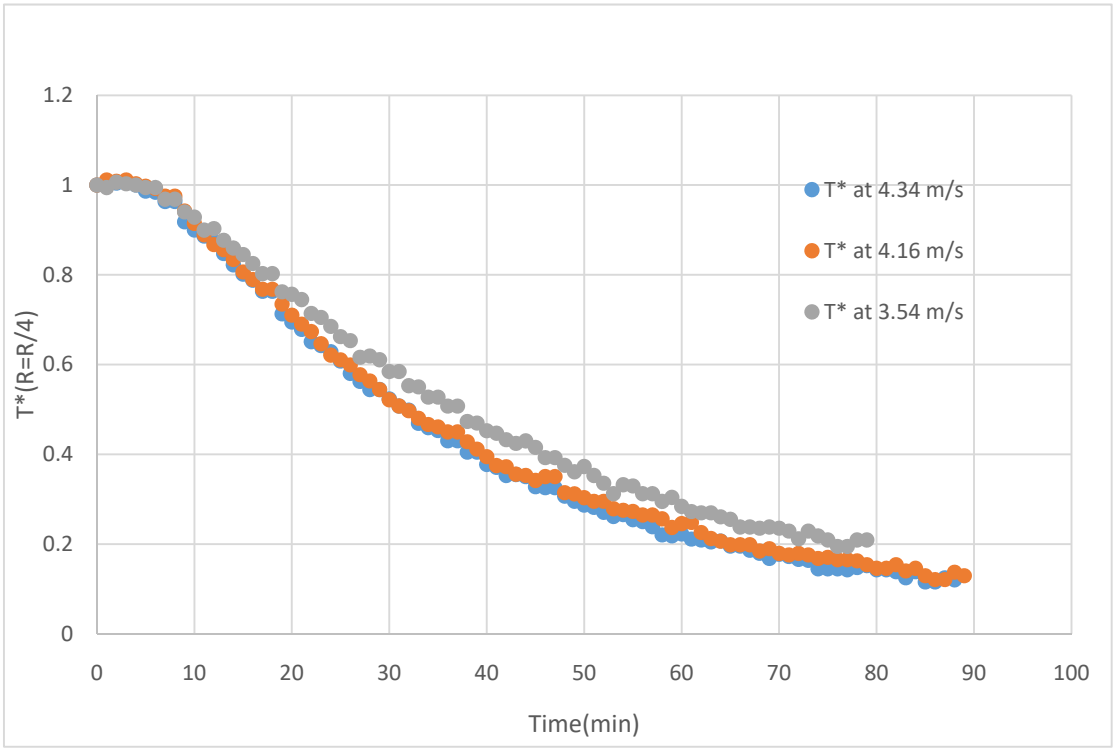

Figure 8. Variationof non-dimensional temperature with time for apple at 3 different velocities.

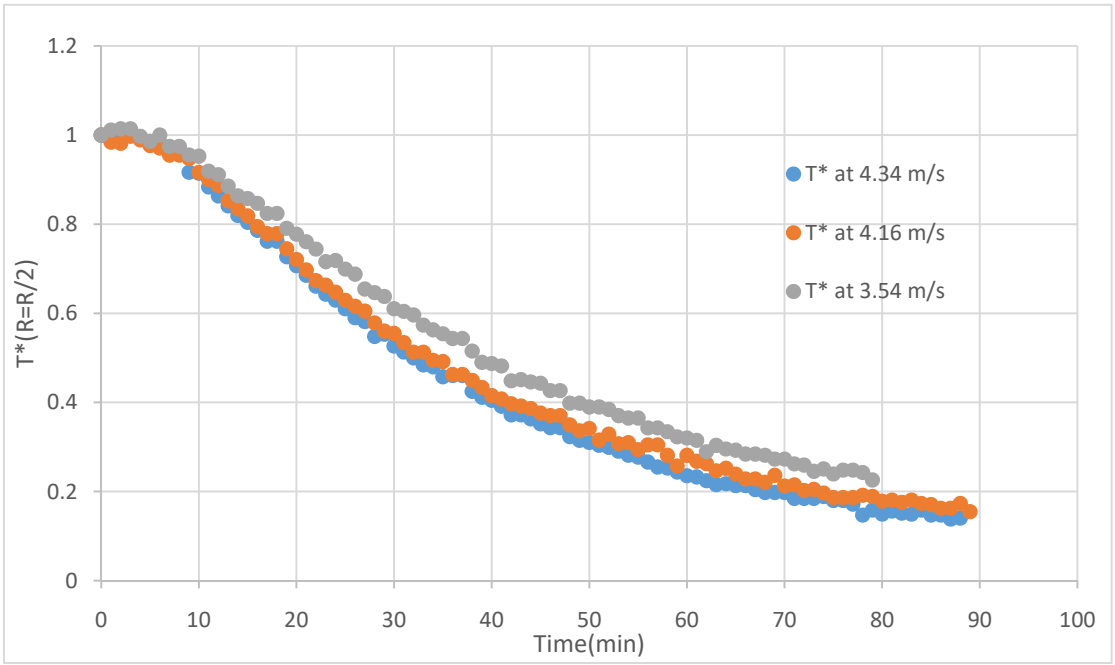

Figure 9. Variationof temperature with time for apple at 3 different velocities.

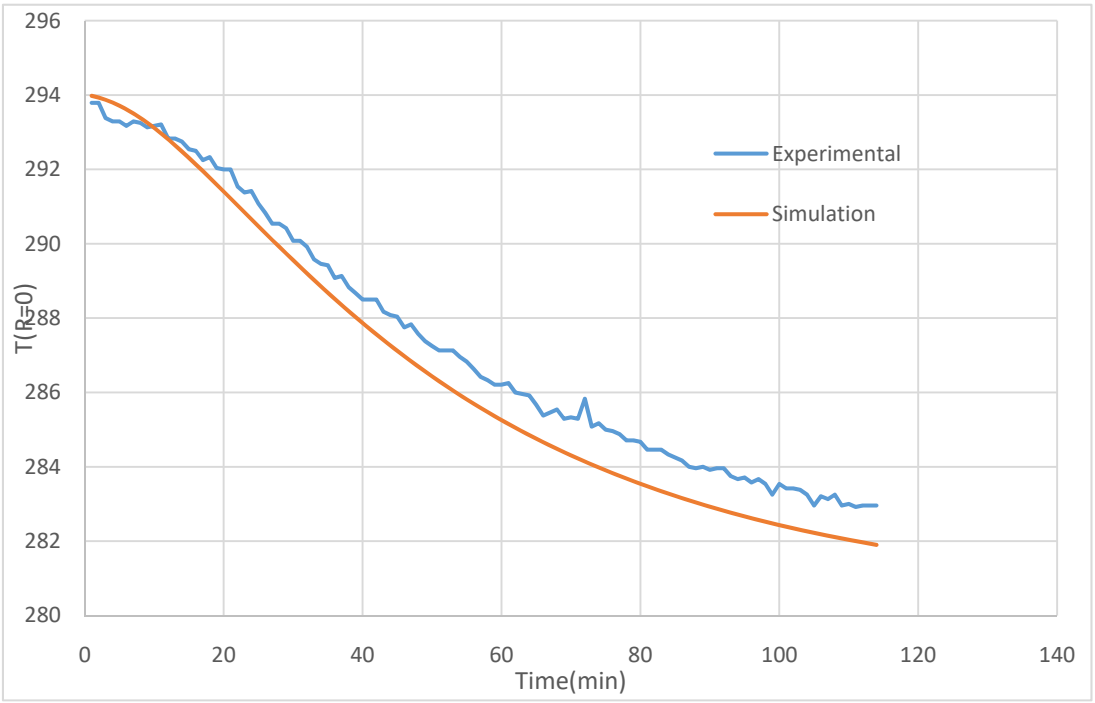

Figure 10. Validation 3-D CFD model with the experimental results for Orange at a velocity of 3.0 m/s.

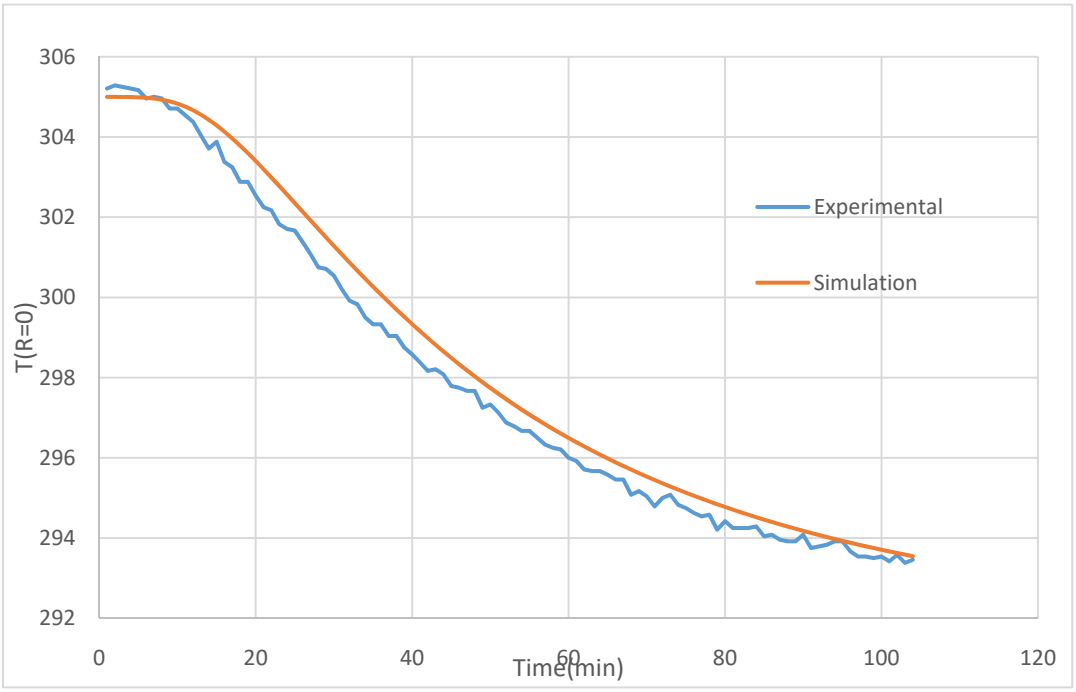

Figure 11. Validation 3-D CFD model with the experimental results for apple at a velocity of 3.0 m/s.

4.2. Simulation results for apple and orange

The Figures 12 and 13 show the variation of volume weighted average temperature (T_{vwa}) with time for apple and orange respectively at different air flow velocities and hence it is clear from Figure 12 that the volume-weighted average temperature of the apple decreases with increasing air-inflow velocity and on increasing the air-inflow velocity, the cooling time significantly reduces. However, for an air-inflow velocity exceeding 2.5 m/s, the cooling and heat transfer fluxes across the sample surface are no longer influenced by air-inflow velocity. Similar is the case for orange as seen in Figure 13 but the critical velocity in this case is 2 m/s.

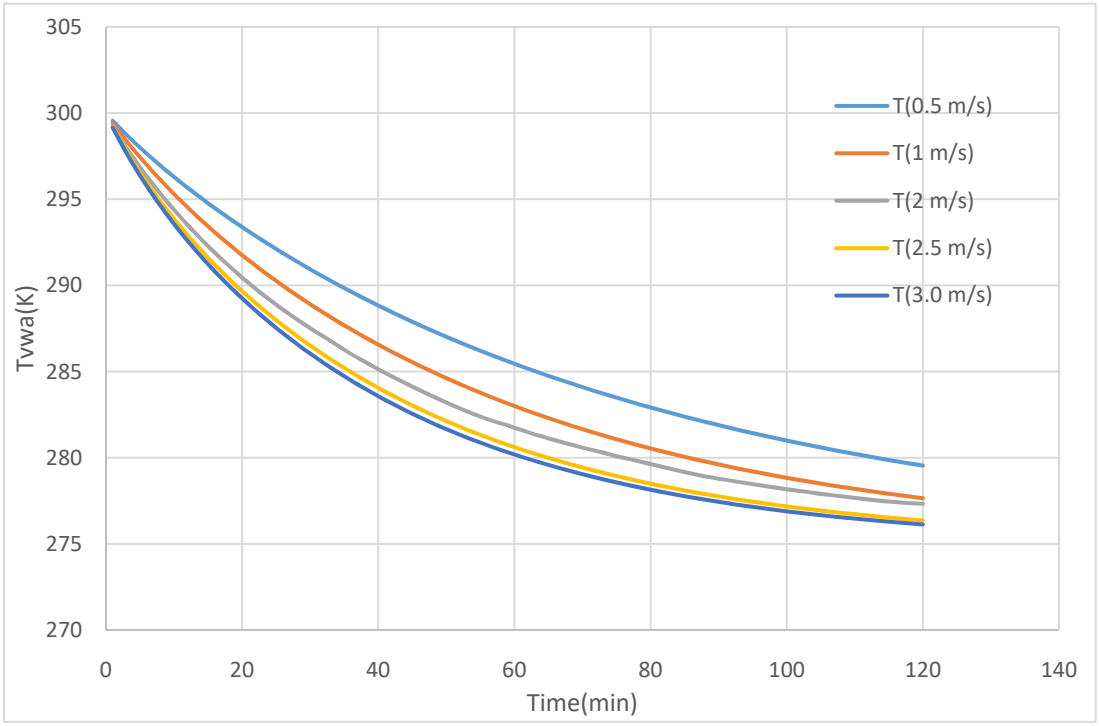

Figure 12. Variation of Volume Weighted Average Temperature(T_{vwa}) with time for apple at different air flow velocities.

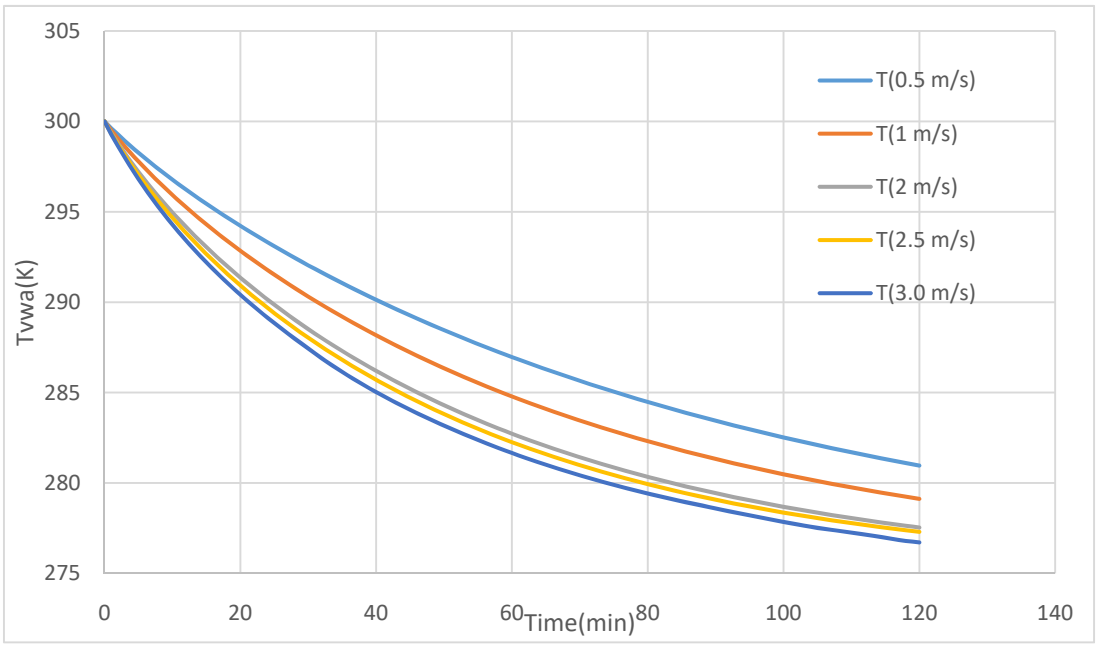

Figure 13. Variation of Volume Weighted Average Temperature with time for orange at different air flow velocities.

4.3. Cooling rates (HCT and SECT)

The equation showing the change of dimensionless temperature in the form of an exponential temperature.

$$T^{*} = J \exp(-C t) \tag{9}$$

where J is the lag factor and C (min^{-1}) is the cooling coefficient.

There are two cooling times which are of importance naming half cooling time (HCT) and seven-eighth cooling time (SECT). The SECT is particularly interesting in commercial-cooling operations because the fruit temperature is then acceptably close to the required storage temperature. At this point, the fruit can be transferred to storage facilities where the remaining heat load can be removed with less energy cost. Regression analyses were done on the dimensionless temperature data in exponential form. From the regression analyses, the cooling coefficient C and lag factor J were calculated. The values obtained for different air-inflow velocities are given in Tables 6 and 7 for apple and orange respectively. As can be seen from Tables 6 and 7, the cooling performance is strongly affected by the increase in the air-inflow velocity. The variation in the lag factor, which is mainly a function of the size, shape and thermal properties of the apple, showed almost no changes for an increase in air-inflow velocity from 0.5 to 3.0 m/s. Therefore, the air-inflow velocity had little influence on the lag factor (C). However, the cooling coefficient increases with increasing air-inflow velocity. The half cooling time and SECT consequently decreases by 45.91% and 44.61%, respectively, for an individual apple with an increase in air-inflow velocity from 0.5 to 3.0 m/s and 44.27% and 43.31% respectively for orange. The SECT is directly proportional to the HCT. The variations in the HCT and SECT, and in particular their decrease with increasing air-inflow velocity, clearly indicate that the air-flow temperature profile and heat transfer conditions around the

individual apple and orange differ for each experiment. However, when the air-inflow velocity exceeds 2.5 m s^{-1}, neither the HCT nor the SECT decrease significantly. Tables 8 and 9 show the comparison of J and C coefficients with and without rotation for apple and orange respectively.

Table 6. J and C coefficients for different air flow velocity for Apple.

Air inflow velocity (m/s)	Eq. (5.3) coefficients $T^* = Jexp(-Ct)$				
	J	C (min^{-1})	R^2	HCT (min)	SECT (min)
0.5	0.9758	0.014	0.9999	47.76	146.78
1	0.9738	0.019	0.9999	35.08	108.04
2	0.9151	0.020	0.9998	30.22	99.53
2.5	0.9520	0.024	0.9999	26.83	84.59
3	0.9543	0.025	0.9999	25.83	81.30

Table 7. J and C coefficients for different air flow velocity for Orange.

Air inflow velocity (m/s)	Eq. (5.3) coefficients $T^* = Jexp(-Ct)$				
	J	C (min^{-1})	R^2	HCT (min)	SECT (min)
0.5	0.9754	0.012	0.9998	55.68	171.21
1	0.9619	0.015	0.9999	43.62	136.03
2	0.9575	0.019	0.9998	34.19	107.15
2.5	0.9474	0.020	0.9997	31.95	101.27
3	0.9595	0.021	0.9998	31.03	97.05

Table 8. Comparison of J and C coefficients with and without rotation for Apple.

Air inflow velocity (m/s)	Eq. (5.3) coefficients $T^* = Jexp(-Ct)$				
	J	C (min^{-1})	R^2	HCT (min)	SECT (min)
2.5	0.9520	0.024	0.9999	26.83	84.59
2.5(with rotation)	0.9714	0.031	0.9998	21.42	66.14

Table 9. Comparison of J and C coefficients with and without rotation for Orange.

Air inflow velocity (m/s)	Eq. (5.3) coefficients $T^* = Jexp(-Ct)$				
	J	C (min^{-1})	R^2	HCT (min)	SECT (min)
2.5	0.9474	0.020	0.9997	31.95	101.27
2.5 (with rotation)	0.9966	0.027	0.9999	25.94	76.89

4.4. Internal conductive heat resistance and external convective thermal resistance

Figure 14 shows the relationship between internal conductive heat resistance and external convective thermal resistance. The ratio of internal conduction resistance and external convective resistance is called the Biot number which is significant in providing a picture of whether lumped system analysis can be applied or not. A less Biot number gives sense that internal conduction resistance is less compared to external convective resistance, less conduction resistance means high thermal conductance and less gradient of temperature within the body. But for a high value of Biot number lumped mass approximation invalid. In the experiment the value of Biot number calculated

is 2.3 which is significantly high to not go for the lumped system analysis. The reason for this was a low thermal conductance of the sample.

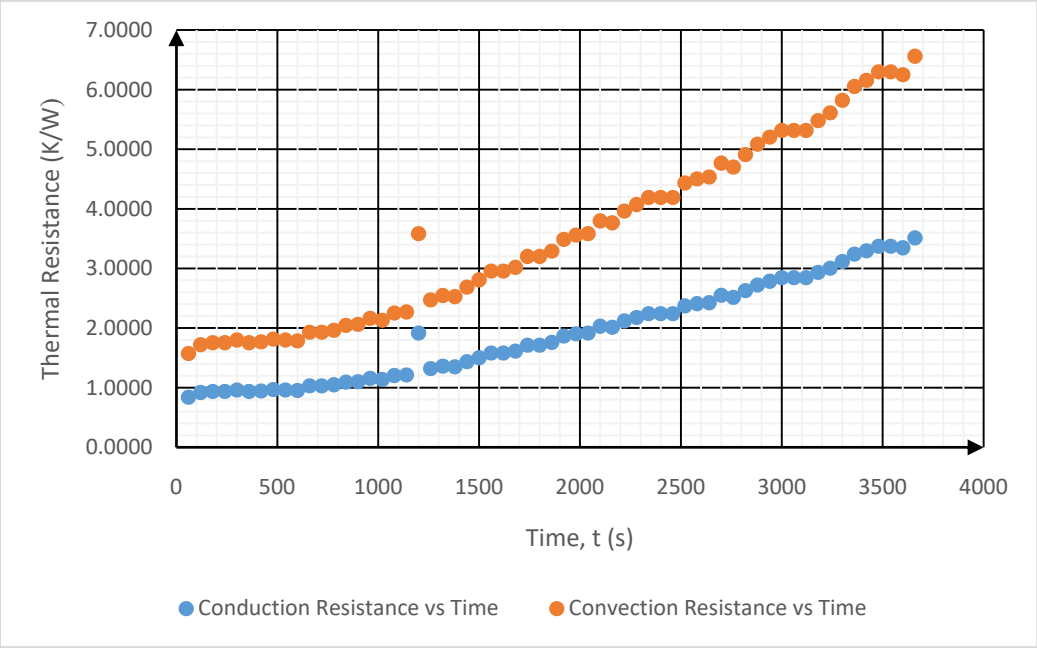

Figure 14. The relationship between internal conductive heat resistance and external convective thermal resistance.

5. Error analysis

To determine the validity of the model the measured and predicted temperatures are compared based on the root-mean-square error (RMSE) and relative deviation (RD).
The RMSE and RD are given by

$$RMSE = \sqrt{\frac{1}{n}\sum_{1}^{n} (E_i - S_i)^2} \tag{10}$$

$$RD = \frac{1}{n}\sum_{1}^{n} \frac{|E_i - S_i|}{E_i} \tag{11}$$

where n = 104 is the number of measurements made for apple and n = 125 for orange, Si is the simulation result at time i and Ei is the measured value. For the CFD model of apple and orange and, the RMSE values for point R = 0 are 0.54 and 0.80 ℃, respectively. The RD values for apple and orange are 1.92% and 4.75%, respectively. The deviations could be considered satisfactory in view of the various parameters controlling the simulation and experiment; e.g., variations in experimental air-inflow velocity, air temperature, thermo physical properties of the sample, and numerical oscillations.

6. Conclusions

Present work establishes a 3D mathematical model of airflow and heat transfer for studying simultaneously the aerodynamic and thermal forced-convection cooling of an individual apple and orange. A 3-D unsteady SST κ-ω mathematical model to simulate the temperature distribution inside the apple and orange with five different air-inflow velocities is proposed. The effects of air-inflow velocity, heat flux and heat transfer coefficient on produce temperature, cooling rate and cooling time are investigated. After carrying out experiments and the simulations at different velocities we found that both values were in very well agreement. This approach allows us to identify the advantages and limitations of each technique. The results indicate that an air inflow velocity exceeding 2.5 m/s for apple and 2.0 m/s for orange does not strongly affect the cooling and heat transfer fluxes through the apple and orange surface. Above their respective critical velocity, neither the HCT nor the SECT significantly decreases, which mean that the extra energy supplied for higher air-flow speed is wasted. This work thus provides a reliable theoretical basis for enhancing the airflow, produce temperature uniformity and minimizing unnecessary energy consumption during forced-convection cooling of produce.

Conflict of interest

The authors declare that they have no known competing financial interests or personal relationships that could have appeared to influence the work reported in this paper.

References

1. Ansari AA, Goyal V, Yahya SM, et al. (2018) Experimental investigation for performance enhancement of a vapor compression refrigeration system by employing several types of water-cooled condenser. *Sci Technol Built Environ* 24: 793–802.
2. Cuevas R, Cheryan M (1978) Thermal conductivity of liquid foods—A review. *J Food Process Eng* 2: 283–306.
3. Rao KN, Narasimham GSVL, Murthy MK (1993) Analysis of heat and mass transfer during bulk hydraircooling of spherical food products. *Int J Heat Mass Transfer* 36: 809–822.
4. Rahman MS, Chen XD, Perera CO (1997) An improved thermal conductivity prediction model for fruits and vegetables as a function of temperature, water content and porosity. *J Food Eng* 31: 163–170.
5. Brosnan T, Sun DW (2001) Precooling techniques and applications for horticultural products—A review. *Int J Refrig* 24: 154–170.
6. Aviara NA, Haque MA (2001) Moisture dependence of thermal properties of sheanut kernel. *J Food Eng* 47: 109–113.
7. Sablani SS, Kasapis S, Rahman MS (2007) Evaluating water activity and glass transition concepts for food stability. *J Food Eng 78*: 266–271.
8. Albayati OAZ, Kumar R, Chauhan G (2007) Forced air precooling studies of perishable food products. *Int J Food Eng*, 3.
9. Ansari FA, Charan V, Varma HK (1984) Heat and mass transfer analysis in air-cooling of spherical food products. *Int J Refrig* 7: 194–197.

10. Ansari FA, Afaq A (1986) New method of measuring thermal diffusivity of spherical produce. *Int J Refrig* 9: 158–160.
11. Ambaw A, Verboven P, Delele MA, et al. (2013) CFD modelling of the 3D spatial and temporal distribution of 1-methylcyclopropene in a fruit storage container. *Food Bioprocess Technol* 6: 2235–2250.
12. Bairi A, Laraqi N, de Maria JG (2007) Determination of thermal diffusivity of foods using 1D Fourier cylindrical solution. *J Food Eng* 78: 669–675.
13. Chuntranuluck S, Wells CM, Cleland AC (1998) Prediction of chilling times of foods in situations where evaporative cooling is significant—Part 1. Method development. *J Food Eng* 37: 111–125.
14. Defraeye T, Lambrecht R, Tsige AA, et al. (2013) Forced-convective cooling of citrus fruit: package design. *J Food Eng* 118: 8–18.
15. Dehghannya J, Ngadi M, Vigneault C (2010) Mathematical modeling procedures for airflow, heat and mass transfer during forced convection cooling of produce: A review. *Food Eng Rev* 2: 227–243.
16. Delele MA, Ngcobo MEK, Getahun ST (2013) Studying airflow and heat transfer characteristics of a horticultural produce packaging system using a 3-D CFD model. Part I: Model development and validation. *Postharvest Biol Technol* 86: 536–545.
17. Denys S, Pieters JG, Dewettinck K (2005) Computational fluid dynamics analysis for process impact assessment during thermal pasteurization of intact eggs. *J Food Prot* 68: 366–374.
18. Hussain T, Ansari S (2020) Free and Forced Air Precooling of Perishable Food Products: Experimental Investigation. *Adv Sci, Eng Med* 12: 517–523.
19. Ghiloufi Z, Khir T (2019) CFD modeling and optimization of pre-cooling conditions in a cold room located in the South of Tunisia and filled with dates. *J Food Sci Technol* 56: 3668–3676.
20. Kumar R, Kumar A, Murthy UN (2008) Heat transfer during forced air precooling of perishable food products. *Biosyst Eng* 99: 228–233.

AIMS Press